Synthesis of microphone array directional patterns

Elouan EVEN
Aalto University
Master's Programme CCIS / AAT

elouan.even@aalto.fi

Abstract

In recent years, the utilization of microphone array systems has surged across diverse fields ranging from telecommunications to audio recording and speech recognition. These systems, comprising multiple microphones arranged strategically, offer enhanced capabilities in capturing sound from different directions and spatially localizing sound sources. Central to the efficacy of these systems is the synthesis of microphone array directional patterns, which dictates the spatial sensitivity profile of the array. This paper presents a comprehensive review of the synthesis techniques employed in shaping these directional patterns, leveraging mathematical methodologies and advanced signal processing algorithms. The synthesis aims to optimize the array's response, enhancing sensitivity to desired sound sources while mitigating interference from noise and undesired sources. With the examination of existing methodologies and emerging trends, this paper elucidates the significance of directional pattern synthesis in augmenting the performance and adaptability of microphone array systems.

1 Introduction

Microphone arrays consist of multiple microphones working in concert. They have become indispensable tools in various fields such as telecommunications, audio recording, and acoustic signal processing. One of the key aspects of their functionality lies in their ability to capture sound from different directions, which is determined by their directional patterns. These patterns illustrate how the array responds to sound sources from various angles.

By understanding and manipulating directional patterns, researchers and practitioners can unlock the full potential of microphone arrays across a spectrum of real-world scenarios.

1.1 Wave Propagation

Sound waves within fluids, like air and water, take the form of longitudinal waves, where the fluid molecules oscillate back and forth in the same direction as the wave travels. This movement creates areas of compression and expansion, known as rarefaction, in adjacent regions. To establish the equation governing the propagation of these waves, we will derive the equations describing the movement of an infinitesimal volume of fluid using Newton's second law of motion.

After making some assumptions about the viscosity of the fluid and considered it ideal, the equation can be denoted as [1]:

$$\nabla^2 x(t, \mathbf{r}) - \frac{1}{c^2} \frac{\delta^2}{\delta t^2} x(t, \mathbf{r}) = 0 \tag{1}$$

where ∇^2 is the Laplacian operator, c is the speed of propagation and x is a function representing the sound pressure at a point in time t and space

$$\mathbf{r} = \begin{bmatrix} x \\ y \\ z \end{bmatrix} \tag{2}$$

We can solve the differential wave Equation 1 by using the separation of variables method. Two solutions can be declined, the first one for a monochromatic plane wave and the second one for a spherical plane wave. In the case of a monochromatic plane wave, the solution is given as :

$$x(t, \mathbf{r}) = A e^{j(\omega t - \mathbf{k} \cdot \mathbf{r})} \tag{3}$$

where A is the wave amplitude, $\omega = 2\pi f$ is the frequency in radians per second, and $\mathbf{k}$ is the wavenumber vector corresponding to the speed and direction of wave propagation, it is defined by :

$$\mathbf{k} = \frac{2\pi}{\lambda} \begin{bmatrix} \sin\theta\cos\phi & \sin\theta\sin\phi & \cos\theta \end{bmatrix} \tag{4}$$

where $\lambda = c/f$ is the wavelength. In the case of a spherical wave, the solution will be :

$$x(t, \mathbf{r}) = -\frac{A}{4\pi r} e^{j(\omega t - kr)} \tag{5}$$

where $k = |\mathbf{k}| = 2\pi/\lambda$ is the scalar wavenumber, and $r = |\mathbf{r}|$ is the radial distance from the source.

Equation 5 shows a decrease in the signal amplitude by increasing the source distance. Sound waves are typically spherical in nature, but they could be considered as plane waves at a certain distance from the source, and this approximation is often used to simplify mathematical analysis. That means that the spherical wave

solution is checked under some distance, in other words, Equation 5 is valid if the source is in the near-field, which corresponds to [2] :

$$r < \frac{2L^2}{\lambda} \tag{6}$$

where L is the length of a linear aperture sonar.

That is why during the whole paper we will work only with plane waves under the far-field condition. In this section, we assumed that the equations are in a homogeneous, lossless medium and we neglect the effects such as dispersion, diffraction, and changes in propagation speed.

1.2 Continuous Apertures

An aperture corresponds to a spatial zone that either transmits (active aperture) or receives (passive aperture) propagating waves. For acoustics, an aperture converts acoustic signals into electrical signals (microphone), or vice-versa (loudspeaker).

1.2.1 Aperture Function

The received signal x_R for an aperture will correspond to the convolution between the signal x and its linear filter with an impulse response a. This will result in :

$$x_R(t, \mathbf{r}) = \int_{-\infty}^{\infty} x(\tau, \mathbf{r}) a(t - \tau, \mathbf{r}) d\tau \tag{7}$$

or, by taking the Fourier transform,

$$X_R(f, \mathbf{r}) = X(f, \mathbf{r}) A(f, \mathbf{r}) \tag{8}$$

where $A(f, \mathbf{r})$ is the aperture function or the sensitivity function, and it defines the response as a function of spatial position along the aperture.

1.2.2 Directivity Pattern

In the case of a linear aperture exposed to planar waves, the response of a receiving aperture varies with the direction of arrival of the waves. By using the solution of the plane wave (Equation 3), it can be proven that the directivity pattern D_R is related to the aperture function A_R [1] by the relation :

$$D_R(f, \alpha) = \mathcal{F}_{\mathbf{r}}\{A_R(f, \mathbf{r})\} \tag{9}$$

$$= \int_{-\infty}^{\infty} A_R(f, \mathbf{r}) e^{j2\pi\alpha\cdot\mathbf{r}} dr \tag{10}$$

where $\mathcal{F}_{\mathbf{r}}\{\cdot\}$ denotes the three-dimensional Fourier transform,

$$\mathbf{r} = \begin{bmatrix} x_a \\ y_a \\ z_a \end{bmatrix} \tag{11}$$

is the spatial location of a point along the aperture, and the direction vector is :

$$\alpha = \frac{1}{\lambda} \begin{bmatrix} \sin(\theta)\cos(\phi) & \sin(\theta)\sin(\phi) & \cos(\theta) \end{bmatrix} \tag{12}$$

where θ and ϕ are respectively the polar angle and the azimuthal angle in a spherical coordinate system. In Figure 1, we have two incident plane waves arriving on an

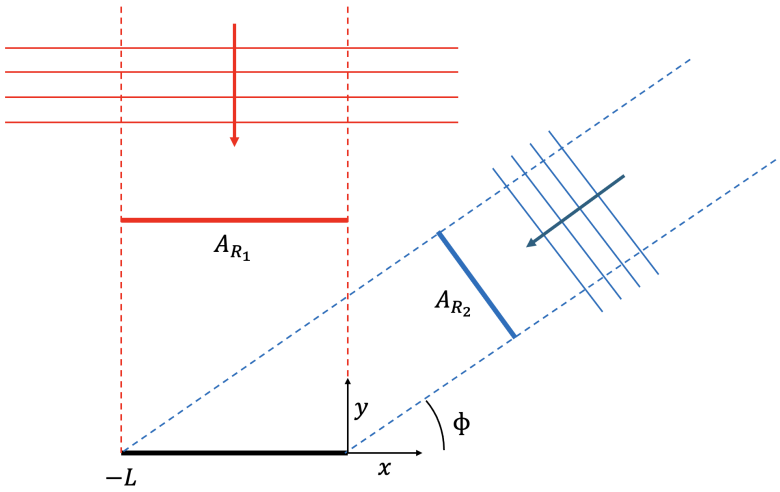

Figure 1: *Aperture representation on an x-y plane from two incident plane waves*

aperture of length L with a normal steering angle for the red plane wave and a steering angle of ϕ for the blue one. We notice that the amount of signal seen by the aperture A_{R_1} is greater than the aperture A_{R_2} due to the steering angle. Therefore, the directivity pattern D_R will be higher with the red planar waves.

1.2.3 Linear Apertures

In this section, we will consider the linear aperture as uniform and frequency-independent. The aperture function may be written as :

$$A_R(x_a) = \text{rect}\left(\frac{x_a}{L}\right) \tag{13}$$

where

$$\text{rect}\left(\frac{x}{L}\right) \widehat{=} \begin{cases} 1 & |x| \leq \frac{L}{2} \\ 0 & |x| > \frac{L}{2} \end{cases} \tag{14}$$

With Equation 9, the resulting directivity pattern is :

$$D_R(f, \alpha_x) = L\,\mathrm{sinc}(\alpha_x L) \tag{15}$$

where

$$\mathrm{sinc}(x) \widehat{=} \frac{\sin(x)}{x} \tag{16}$$

We can notice that the directivity pattern reaches zero when $\alpha_x = m\lambda/L$, where m is an integer and $\alpha_x = \frac{\sin\theta\cos\phi}{\lambda}$ is the x component of the α vector. The main lobe refers to the area of the directivity pattern in the range $-\lambda/L \leq \alpha_x \leq \lambda/L$. The beam width designates its extent with a value of $2\lambda/L$ also equal in frequency at $2c/fL$. We can conclude that the beamwidth and the frequency will be inversely proportional.

To examine the effectiveness of the directivity pattern over varying angles of arrival we need to consider the normalized directivity pattern as :

$$D_N(f, \alpha_x) = \frac{D_R(f, \alpha_x)}{D_{\max}} = \mathrm{sinc}(\alpha_x L) \tag{17}$$

where $D_{max} = L$ is the maximum possible value of the directivity pattern.

For a better understanding of the physical significance of α_x, we will consider a horizontal directivity pattern, i.e. $\theta = \frac{\pi}{2}$, implying $\alpha_x = \frac{\cos\phi}{\lambda}$. That leads to the following equation :

$$D_N(f, \frac{\pi}{2}, \phi) = \mathrm{sinc}\left(\frac{L}{\lambda}\cos\phi\right) \tag{18}$$

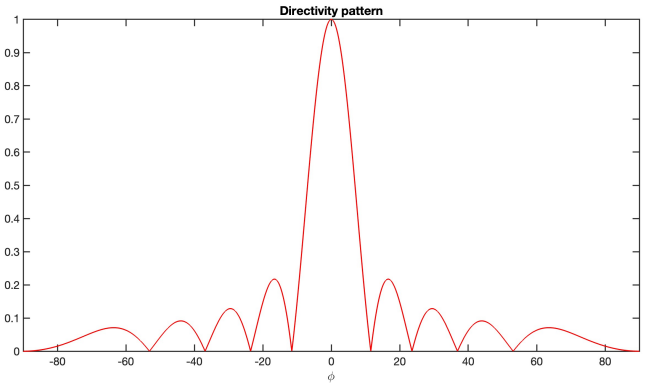

Figure 2: *Horizontal directivity pattern for* $\frac{L}{\lambda} = 5$

Figure 2 well illustrates the properties of the directivity pattern with a ratio of $\frac{L}{\lambda} = 5$, the bandwidth in this case is equal to $2 * \frac{\lambda}{L}\frac{180}{\pi} = 23°$.

To observe the evolution of the ratio $\frac{L}{\lambda}$, we plot Figure 3. We notice that the more the ratio gets important the narrower the main lobe gets. We also notice the apparition of several secondary lobes at a higher ratio.

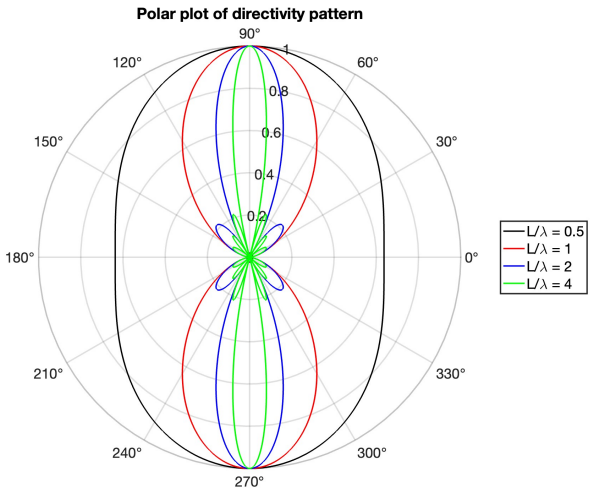

Figure 3: *Polar plot of directivity pattern*

1.3 Discrete Sensor Arrays

In practice, an aperture is not continuous but rather excited at a finite number of discrete points. To define a sensor array, we use the superposition principle of multiple sensor responses.

1.3.1 Linear Sensor Arrays

Considering a linear array of N elements and using the superposition principle, we can express the complex frequency response of the array as [3]:

$$A(f, x_a) = \sum_{n=1}^{N} w_n(f) e_n(f, x_a - x_n) \tag{19}$$

where w_n is the complex weight for element n, e_n is the complex frequency response of the sensor n and x_n is its spatial position on the x-axis. The directivity pattern for a linear, equally spaced array of identical sensors is :

$$D(f, \phi) = \sum_{n=1}^{N} w_n(f) e^{j\frac{2\pi f}{c} nd\cos\phi} \tag{20}$$

where d is the distance between all successive elements.

Using all of the above assumptions, the effective length of the sensor array used is $L = Nd$. From a physical point of view, the actual physical length of the array will be $L = (N-1)d$.

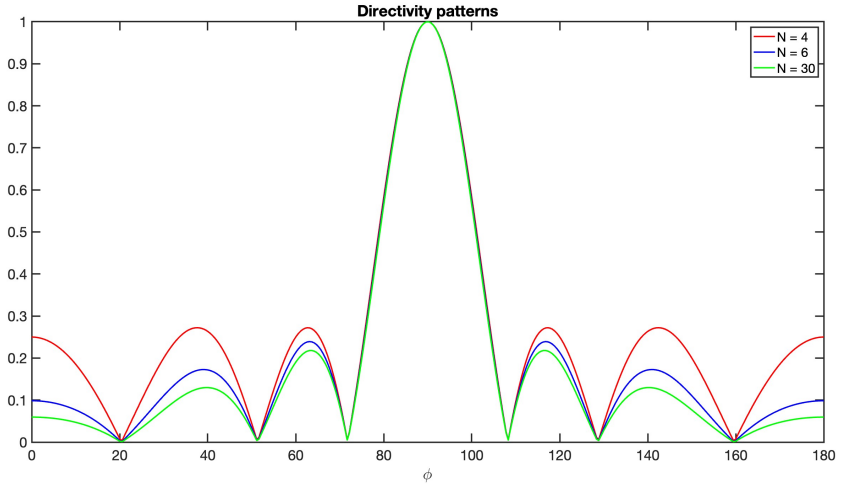

Figure 4: *Directivity pattern with different numbers of sensors (f=1kHz, L=1m)*

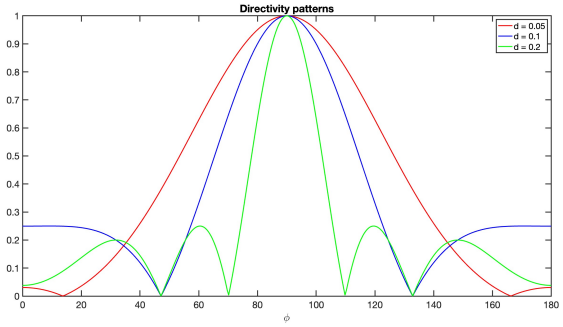

Figure 5: *Directivity pattern with different distances between sensors (f=1kHz, N=5)*

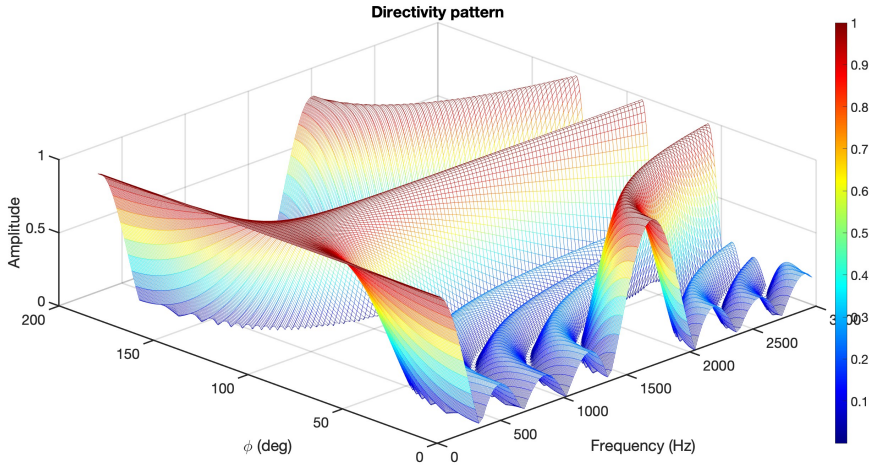

Figure 6: *Directivity pattern for $f \in [0, 3000]Hz$ (N=5, d=0.2)*

From the equation 20, we see that the directivity pattern depends upon three parameters: the number of array elements N, the inter-element spacing d, and the frequency f. We will plot three figures and vary each parameter to observe the effect on the directivity pattern.

Thanks to Figure 4, we observe that the sidelobe level decreases with increasing spatial sampling frequency. In conclusion, the more sensors we use, the lower the sidelobe level. In Figure 5, we can notice that the beam width is inversely proportional to the array length. Finally, Figure 6 shows the beamwidth decreasing for an increasing frequency.

1.3.2 Spatial Aliasing

The Nyquist–Shannon sampling theorem defines the minimum frequency required to avoid aliasing. There are two types of aliasing, temporal sampling aliasing and spatial sampling aliasing.

To avoid grating lobes, in the directivity pattern for the temporal sampling, the signal must be sampled at a rate f_s such that :

$$f_s = \frac{1}{T_s} \geq 2f_{max} \tag{21}$$

where f_{max} is the maximum frequency component in the signal's frequency spectrum. In the case of spatial sampling, the requirement is [3] :

$$f_{x_s} = \frac{1}{d} \geq 2f_{x_{max}} \tag{22}$$

where f_{x_s} is the spatial sampling frequency in samples per meter and $f_{x_{max}}$ is the highest spatial frequency component in the angular spectrum of the signal. Furthermore, we know that :

$$f_{x_{\max}} = (f_x s)_{\max} = \left| \frac{\sin\theta\cos\phi}{\lambda} \right|_{max} = \frac{1}{\lambda_{\min}} \tag{23}$$

Considering the maximum value of $f_{x_{max}}$ the requirement becomes:

$$d < \frac{\lambda_{min}}{2} \tag{24}$$

where λ_{min} is the minimum wavelength in the signal of interest. Equation 24 is known as the spatial sampling theorem and must be adhered to prevent the occurrence of spatial aliasing in the directivity pattern of a sensor array.

We can see this kind of aliasing in Figure 6 where $f_{x_{max}} = 850Hz$. The peak at 1500 Hz corresponds to this aliasing frequency. In this case, we should have taken only the part under 850Hz for better reliability.

1.3.3 Array Gain and Directivity Factor

The main interest of a sensor array is the improvement of the signal-to-noise ratio to a unique reference sensor. In order to compare both we measure the array gain G_a expressed as [4]:

$$G_a = \frac{G_d}{G_n} \tag{25}$$

where G_d is the gain to the desired signal and G_n is the average gain to all noise sources. In the case of a diffuse noise field, the array gain is also known as the factor of directivity

$$G_a(f, \theta_0, \phi_0) = \frac{|D(f, \theta_0, \phi_0)|^2}{\frac{1}{4\pi} \int_0^{2\pi} \int_0^{\pi} |D(f, \theta, \phi)|^2 \sin\theta \, d\theta \, d\phi} \tag{26}$$

where the desired source is located in the direction (θ_0, ϕ_0).

1.4 Beamforming

For the far-field horizontal directivity pattern of a linear sensor array, we have :

$$D(f, \alpha_x) = \sum_{n=1}^{N} w_n(f) e^{j2\pi\alpha_x nd} \tag{27}$$

where in general w_n can be expressed in terms of its magnitude a_n and phase ϕ_n components as :

$$w_n(f) = a_n(f) e^{j\varphi_n(f)} \tag{28}$$

Modifying the amplitude weights has an impact on the shape of the directivity pattern and at the same time modifying the phase weights impacts the angular location of the response's main lobe. The main goal before applying beamforming techniques is to determine the complex sensor weights w_n.

2 Beamforming Techniques

Beamforming, a pivotal technology in wireless communications, employs arrays of antennas to enhance signal transmission. Fixed beamforming techniques involve predetermined signal adjustments to optimize directionality and reduce interference. Conversely, adaptive beamforming adapts dynamically to changing conditions, dynamically adjusting phase and amplitude to optimize signal reception. In our case, we will focus more on fixed beamforming with data independence.

2.1 Noise Fields

There are three main categories of noise fields for microphone array applications. These categories are characterised by the degree of correlation between noise signals at different spatial locations. A commonly used measure of the correlation is the coherence, which is defined as [3]:

$$\Gamma_{ij}(f) = \frac{\Phi_{ij}(f)}{\sqrt{\Phi_{ii}(f)\Phi_{jj}(f)}} \tag{29}$$

where Φ_{ij} is the cross-spectral density between signals i and j. The three categories of noise fields are the :

- Coherent noise fields, where noise signals propagate to the microphones directly from their sources. The noise between microphones will be strongly correlated. That results in $|\Gamma_{ij}(f)|^2 \approx 1$.
- Incoherent noise field, where noise measured at any given spatial location is uncorrelated with the noise measured at all other locations. That results in $|\Gamma_{ij}(f)|^2 \approx 0$.
- Diffuse noise field, where noise of equal energy propagates in all directions simultaneously. That results in $\Gamma_{ij}(f) = \text{sinc}\left(-\frac{2\pi f d_{ij}}{c}\right)$ where d_{ij} is the distance between sensors i and j.

2.2 Classical Beamforming

2.2.1 Delay-sum Beamforming

Delay-sum beamforming consists of phase weight to the input channels. This will steer the main lobe of the directivity pattern to a desired direction. In a delay-sum beamformer, the phase weighting is frequency-dependent contrary to the amplitude weighting. In order to obtain the correct phase weight, we have to consider the time τ_n the plane wave takes to travel between the reference sensor and the n^{th} sensor:

$$\tau_n = \frac{(n-1)d\cos\phi'}{c} \tag{30}$$

where ϕ' corresponds to the steering angle of the main lobe of the directivity pattern. By knowing that the delay for the nth sensor can also be expressed as :

$$\tau_n = \frac{\varphi_n}{2\pi f} \tag{31}$$

And by applying this time delay to the negative phase shift we obtain the following phase weights :

$$\varphi_n = \frac{-2\pi f(n-1)d\cos\phi'}{c} \tag{32}$$

In a delay-sum beamformer, the phase weighting is frequency-dependent contrary to the amplitude weighting. Usually, each channel is given an equal amplitude weighting in the summation, so that the directivity pattern demonstrates unity gain in the desired direction, which gives :

$$w_n(f) = \frac{1}{N} e^{j\frac{-2\pi f(n-1)d\cos\phi'}{c}} \tag{33}$$

We obtain finally the following directivity pattern :

$$D(f,\phi) = \sum_{n=1}^{N} e^{j\frac{2\pi f(n-1)d(\cos\phi - \cos\phi')}{c}} \tag{34}$$

In our case, the directivity pattern's main lobe has moved to the direction $\phi = \phi'$.

Finally, we can express the array output as the sum of the weighted channels and we obtain :

$$y(f) = \frac{1}{N}\sum_{n=1}^{N} x_n(f) e^{j\frac{2\pi f(n-1)d\cos\phi'}{c}} \tag{35}$$

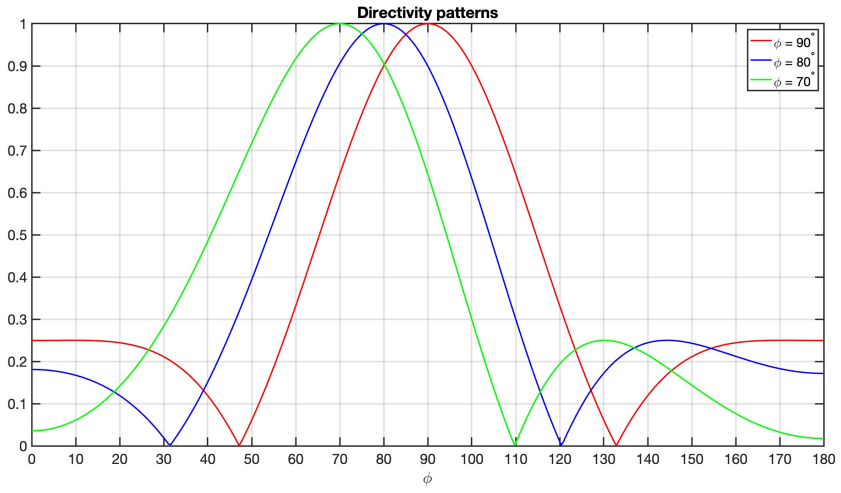

Figure 7: *Directivity pattern with steering angles (f=1kHz, N=5, d=0.1m)*

In Figure 7, we can see the evolution of the steering over the main lobe following the value ϕ in input.

2.2.2 Filter-sum Beamforming

The delay-sum beamformer is in fact just a particular case of the filter sum beamformers, in which both the amplitude and phase weights are frequency dependent. The weight will then correspond to Equation 28.

2.2.3 *Sub-array Beamforming*

We saw in the section "Spatial Aliasing" that the frequency has to respect the spatial sampling theorem which limits the frequency domain to only some bandwidth. The idea of sub-array beamforming is to cover broadband frequency signals. To do so, the method is to implement the array as a series of sub-arrays, which are themselves linear arrays with uniform spacing. Each sub-array will be designed to give the desired frequency range. In addition, to ensure the sidelobe level remains the same across different frequency bands, the number of elements in each sub-array should remain the same to keep the same resolution. Each sub-array is restricted to a different frequency range by applying band-pass filters, and the overall broad-band array output is formed by recombining the outputs of the band-limited sub-arrays.

To obtain the total output y, we have to start by summing the weighted channels for each sub-array s and apply them to a band-pass filter with specified frequencies for each sub-band as :

$$y_s(f) = \sum_{n=1}^{N} w_{s,i}(f) x_i(f) \tag{36}$$

where x_i is the input to channel i of the array, and N is the number of microphones in the array with only the microphones from the sub-array s being sum. In general, we use a delay-sum beamforming technique for the weights. The final step is to sum all of the S sub-arrays by :

$$y(f) = \sum_{s=1}^{S} y_s(f) \tag{37}$$

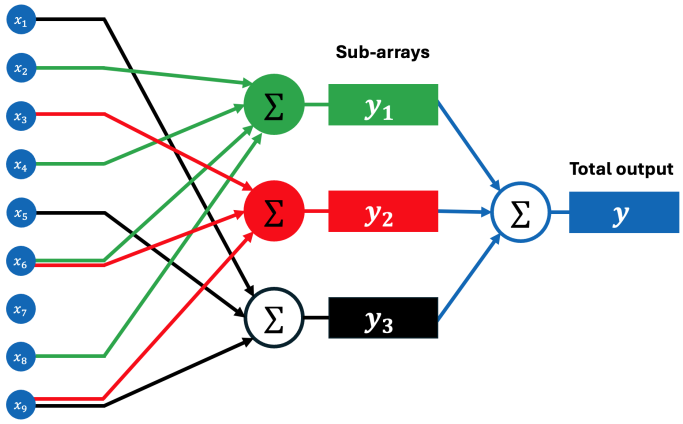

Figure 8: *Sub-array diagram*

Figure 8 shows each step of the method. Considering all sensors are equally spaced and considering the spatial aliasing, we can attribute the first sub-array to high frequency, the second one to the medium, and the last one to low frequency. In this case, we tried to keep approximately the same number of sensors in each sub-array.

2.3 Superdirective Beamforming

A superdirective beamformer can emphasize the properties of a simple linear array by reducing the spacing between the sensors. To verify this improvement, we will maximize the array gain (Equation 26). Considering $\mathbf{w}$ is the filter-sum weight vector, $\mathbf{d}$ the propagation vector, we can formulate the horizontal directivity pattern in matrix notation as [5]:

$$D(f,\phi) = \sum_{n=1}^{N} w_n(f) e^{j\frac{2\pi f}{c}(n-1)d\cos\phi} \tag{38}$$

$$= \mathbf{w}(f)^H \mathbf{d}(f) \tag{39}$$

where $(\cdot)^H$ denotes matrix transpose conjugate. By implementing Equation 26 in Equation 39 we obtain :

$$G_a(f,\theta_0,\phi_0) = \frac{|\mathbf{w}(f)^H \mathbf{d}(f)|^2}{\mathbf{w}(f)^H \mathbf{\Gamma}(f) \mathbf{w}(f)} \tag{40}$$

where $\mathbf{\Gamma}$ is the diffuse noise field defined as :

$$\mathbf{\Gamma}(f) = \frac{1}{4\pi} \int_0^{2\pi} \int_0^{\pi} \mathbf{d}(f)\mathbf{d}(f)^H \sin\theta \, d\theta \, d\phi \tag{41}$$

2.3.1 Unconstraint Array Gain

Superdirective beamformers have to stay the most general as possible. In this part, the objective is to optimize the array gain by calculating the best weight vector $\mathbf{w}$, i.e. :

$$max_{\mathbf{w}} \frac{|\mathbf{w}^H \mathbf{d}|^2}{\mathbf{w}^H \mathbf{\Gamma} \mathbf{w}} \tag{42}$$

The solution is :

$$\mathbf{w} = \beta \Gamma^{-1} \mathbf{d} \tag{43}$$

where β is an arbitrary complex constant. Choosing β to produce a unity signal response with zero phase shift so that $\mathbf{w}^H \mathbf{d} = 1$ gives :

$$\mathbf{w} = \frac{\mathbf{\Gamma}^{-1} \mathbf{d}}{\mathbf{d}^H \mathbf{\Gamma}^{-1} \mathbf{d}} \tag{44}$$

This will result in an array gain equal to :

$$G_a = \mathbf{d}^H \mathbf{\Gamma}^{-1} \mathbf{d} \tag{45}$$

2.3.2 White Noise Gain

In practice, the previous section can lead to an undesirable gain of incoherent noise due to electrical sensor noise and errors in microphone spacing. To robustify the solution we consider that the noise is spatially white or uncorrelated from sensor to sensor, Γ becomes the identity matrix. The array gain becomes the *white noise gain* [5] G_w, express as :

$$G_w = \frac{|\mathbf{w}^H \mathbf{d}|^2}{\mathbf{w}^H \mathbf{w}} = \delta^2 \leq M \tag{46}$$

where the constraining value δ^2 must be chosen less than or equal to the maximum possible white noise gain M for the problem to be self-consistent. The solution of this equation is an analogy to the Equation 44 :

$$\mathbf{w} = \frac{[\Gamma + \varepsilon I]^{-1}\mathbf{d}}{\mathbf{d}^H[\Gamma + \varepsilon I]^{-1}\mathbf{d}} \tag{47}$$

where ε is the Lagrange Multiplier and is adjusted to satisfy the white noise gain constraint.

3 Simulation

To apply the theory to a practice case, we model a linear array sensor and simulate a random noise arriving from one direction. In this simulation, we will focus on the filter-sum beamforming method.

We will position the sensors along the x-axis equally spaced d and the noise will arrive on each sensor with a time delay depending on the direction of arrival ϕ. To create a real environment we will add white noise with a signal-to-noise ratio equal to zero.

Considering the parameter as $N = 10$, $d = 0.5$, $\phi = 80°$, $F_s = 8kHz$, $c = 1500m.s^{-1}$ (we consider here the underwater celerity) and a total duration of the signal of 5 seconds.

Figure 9 shows the energy from a time window of the signal. To have a temporal view, we need to stage the average energy over the useful frequency. Knowing that the aliasing frequency is equal to 1500Hz and to reduce the noise in the low frequency, the average energy is taken between 500Hz and 1500Hz. The choice of a low cut frequency is totally subjective by looking at Figure 9. Best approximation and amplification at low frequency are developed in [6].

We obtain the results in Figure 10 by overlapping the windows. We notice that the main lobe is well-centered around $\phi = 80°$match with the incoming angle of the noise. We can also note that by taking the average energy over frequency the other lobes will cancel each other.

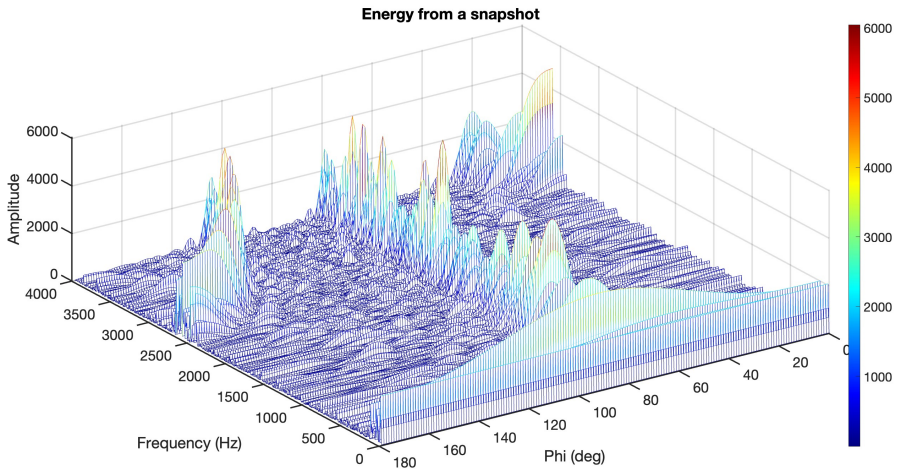

Figure 9: *Energy from a snapshot*

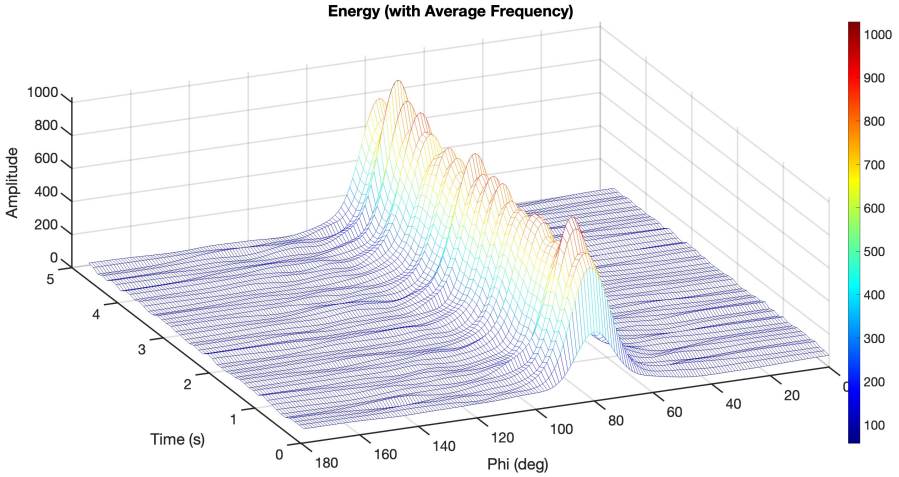

Figure 10: *Energy of the signal-averaged on frequency*

4 Conclusion

Various beamforming techniques have been meticulously examined to precisely discern the direction of arrival of sound sources within a 2D environment using a linear sensor array. It becomes evident that the performance of these techniques is intricately tied to directional patterns, thus directly influenced by factors such as the number of sensors, inter-element spacing, and observed frequency. The filter-sum beamforming technique is tested and the results show accurate results in the direction of the source.

References

[1] L. Ziomek, *Fundamentals of Acoustic Field Theory and Space-Time Signal Processing (1st ed.)*. 1994.

[2] B. Steinberg, *Principles of Aperture and Array System Design: Including Random and Adaptive Arrays*. A Wiley-Interscience publication, Wiley, 1976.

[3] I. McCowan, *Microphone Arrays : A Tutorial*. 2001.

[4] D. Cheng, "Optimization techniques for antenna arrays," *Proceedings of the IEEE*, vol. 59, no. 12, pp. 1664–1674, 1971.

[5] H. Cox, R. Zeskind, and M. Owen, "Robust adaptive beamforming," *IEEE Transactions on Acoustics, Speech, and Signal Processing*, vol. 35, no. 10, pp. 1365–1376, 1987.

[6] S. Delikaris-Manias, C. A. Valagiannopoulos, and V. Pulkki, "Optimal directional pattern design utilizing arbitrary microphone arrays: A continuous-wave approach," in *Audio Engineering Society Convention 134*, May 2013.